ESI

Direct CO$_2$ capture from simulated and ambient air over silica-rich MIL-101(Cr)

Vaishnavi Kulkarni, [†] and Sanjay Kumar Singh[*,†]

†Department of Chemistry, Indian Institute of Technology Indore, Simrol, Indore 453552, India

e-mail: sksingh@iiti.ac.in (SKS)

Table of Contents

1. Experimental Section

1.1 Materials

Terephthalic acid (H$_2$BDC, 98%), chromium (III) nitrate nonahydrate (Cr(NO$_3$)$_3$·9H$_2$O, 98%), nitric acid (68–70%), acetone (≥ 99%), hydrochloric acid (36.5–38%), and distilled water were provided by Merck. Anhydrous ethanol, used as a solvent, was purchased from Changshu Hongsheng Fine Chemical Company. All these materials and reagents were utilized without any further purification. Rice husk ash (RHA) was supplied by Nishant Enterprises India and pre-treated before use. The high purity N$_2$ (99.99%) and 400 ppm CO$_2$ in He (99.99%) were supplied by Inox air products Pvt. Ltd. and Sigma gases and services, India, respectively for the adsorption measurement.

2. Characterization

The powder X-ray diffraction (P-XRD) patterns of the adsorbents are obtained with a Rigaku Smart Lab automated powder X-ray diffractometer with monochromatic Cu Kα radiation (λ = 0.154 nm) and a 0.01° step size over a 2θ range of 2° to 30°. Fourier transform infrared spectroscopy (FTIR) is used to evaluate the vibrational properties of various functional groups present in the adsorbents and is acquired in the wavenumber range of 4000–500 cm^{-1} using a spectrometer with an attenuated total reflectance (FTIR/ATR 229 model FTIR-STD-10, PerkinElmer, MA, USA). Further, to investigate the thermal stability of the analysed adsorbents, a thermogravimetric study (TGA) is done from 25 °C to 800 °C at a heating rate of 5 °C min^{-1} in N$_2$ environment using a Mettler-Toledo TGA/DSC-1 thermal analyzer. Carl Zeiss Supra-55 and an EDS Oxford instrument (X-Max, energy-dispersive X-ray spectrometer) are used to capture FESEM images and EDS spectra, respectively. Similarly, an FEI Talos 200S transmission electron microscope with a 200 kV Field Emission Gun is used to obtain EDS elemental mapping and transmission electron microscopic (TEM) images. Inductively coupled plasma atomic emission spectroscopy (ICP-AES) analysis is performed on ARCOS, simultaneous ICP spectrometer (make: SPECTRO, analytical instruments GmbH, Germany) (spectral wavelength range: 130 nm to 770 nm). The Raman spectra is acquired using a Labram HR evolution Raman spectrometer (Horiba Jobin Yvon) with an argon-ion laser (λ= 532 nm). The textural parameters (specific surface area, pore volume, and pore size distribution) at −196°C are measured using a Quantachrome Autosorb iQ2 TPX automated gas sorption system. The Brunauer–Emmett–Teller (BET) equation was used to calculate the specific surface areas of the adsorption data for the relative pressure (P/P$_0$) range of 0.05–0.20. The

total pore volume (V_{total}) was calculated from the quantity of adsorbed N_2 at $P/P_0 = 0.99$ using the single point adsorption method. Micropore volume (V_{micro}) was calculated using the t-plot method, whereas ultra-micropore volume ($V_{ultramicro}$) was calculated using the NLDFT method for pores smaller than 0.7 nm.

3. Evaluation of CO_2 adsorption performance of powder and structured RHA-MIL-101(Cr)

The recovery of CO_2 adsorption capacity of pelletized and granular form of RHA-MIL-101(Cr)-IV as compared to the powdered adsorbent is calculated using Eq. S1.[1]

$$\text{Recovery (\%)} = \frac{CO_2 \text{ adsorption capacity of pelletized/granulated adsorbent}}{CO_2 \text{ adsorption capacity of powdered adsorbent}} \times 100$$

(S1)

4. Evaluation of heat of desorption of CO_2

The heat of desorption of CO_2-saturated RHA-MIL-101(Cr) is measured using differential scanning calorimetry (DSC) according to the procedure outlined by Su et al.[14] and Gray et al.[15] In this method, a CO_2-saturated RHA-MIL-101(Cr) sample weighing between 0.03 to 0.09 g is placed in an aluminum pan. The pan is pierced with a pinhole, and then it is mounted in a DSC analyzer (Perkin Elmer 8000). The sample is initially held at 30 °C for 1 minute to stabilize the signal, followed by heating from 30 °C to 110 °C at a rate of 5 °C/min in the presence of a dry nitrogen atmosphere (20 mL/min). This heating process allows the CO_2 retained in the sample to be desorbed. Prior to the experiment, a blank run and baseline correction are performed, and the heat of desorption is analyzed from the DSC profile by measuring the area corresponding to the endothermic peak using Pyris™ software built into the DSC machine. The temperature calibration of the DSC is carried out using the melting point of an indium sample (156.60 °C).
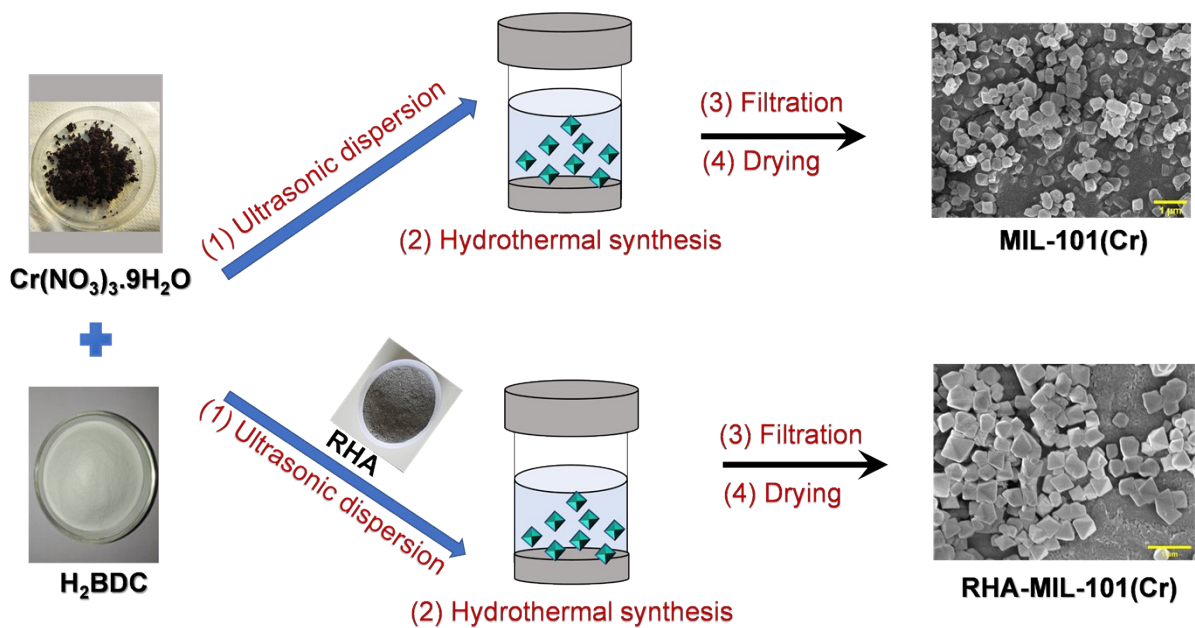
Scheme S1. Schematic representation for the synthesis of RHA-MIL-101(Cr).
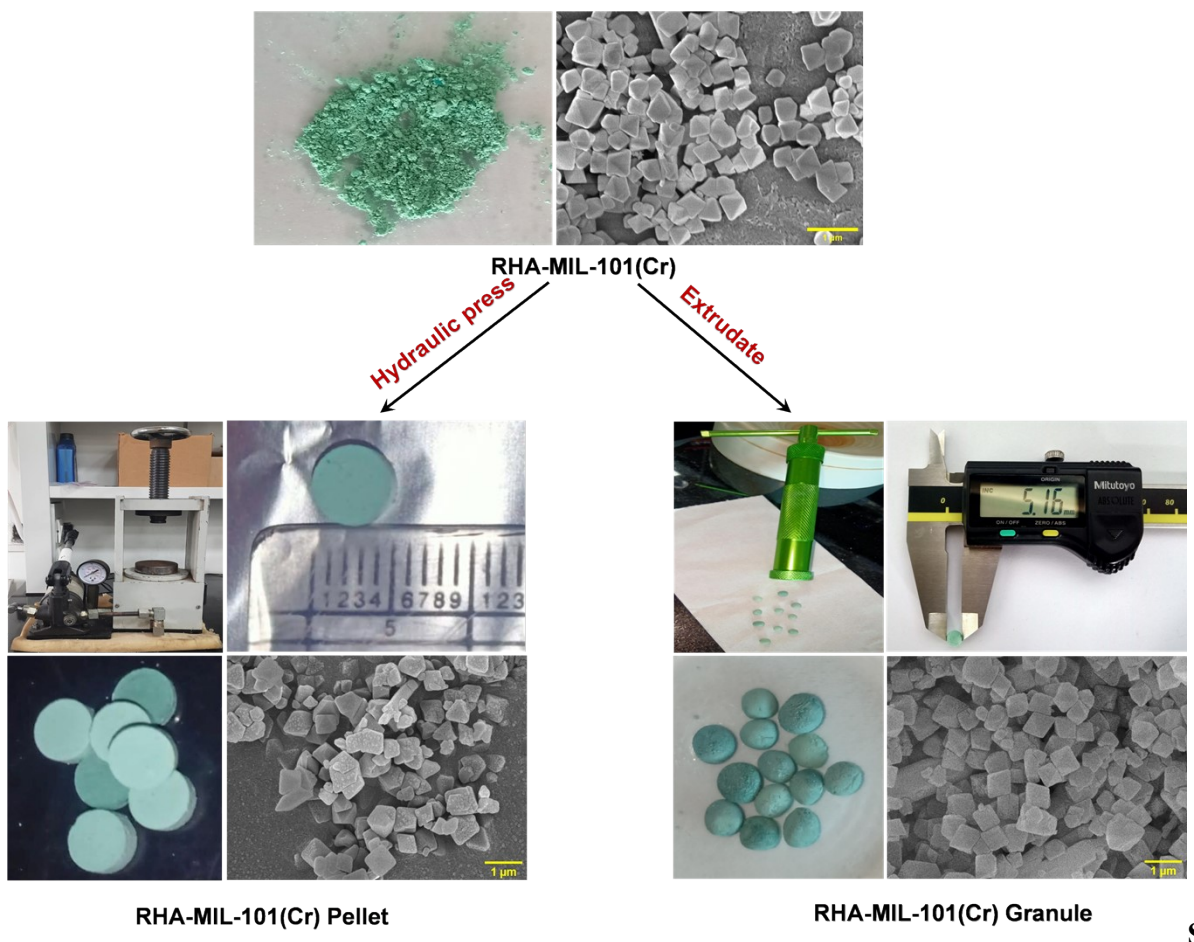
Scheme S2. Schematic representation for the synthesis of RHA-MIL-101(Cr) pellet and RHA-MIL-101(Cr) granule.
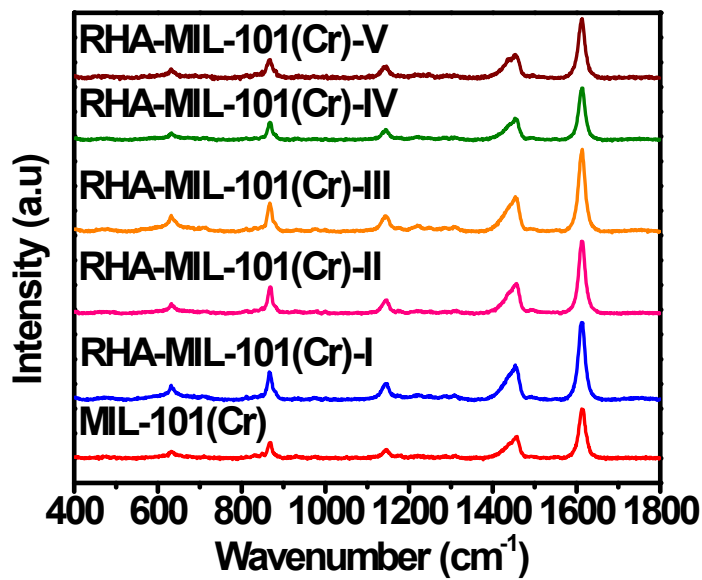
Figure S1. Raman spectra of MIL-101(Cr) and RHA-MIL-101(Cr).
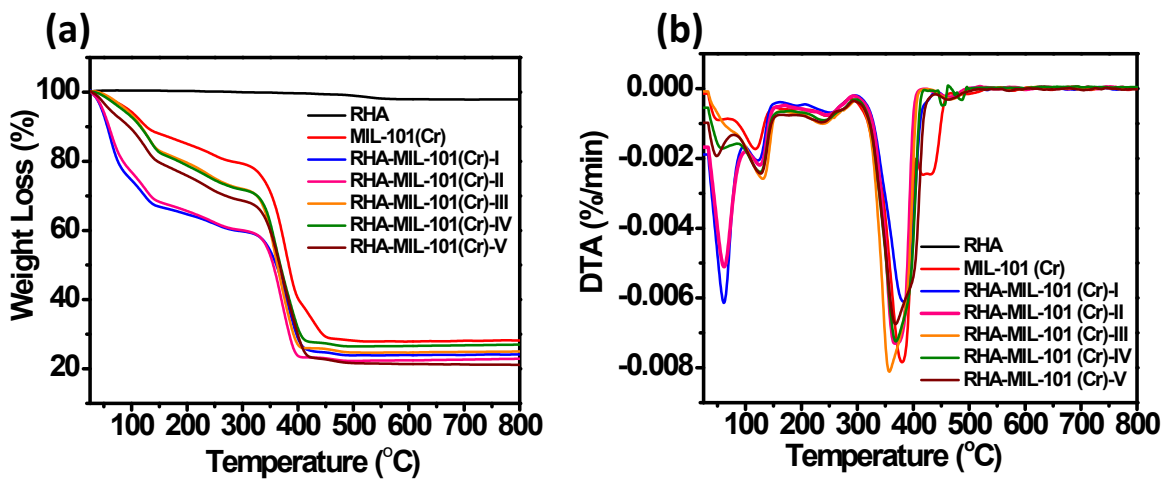
Figure S2. (a) TGA and (b) DTA curves of RHA, MIL-101(Cr) and RHA-MIL-101(Cr).
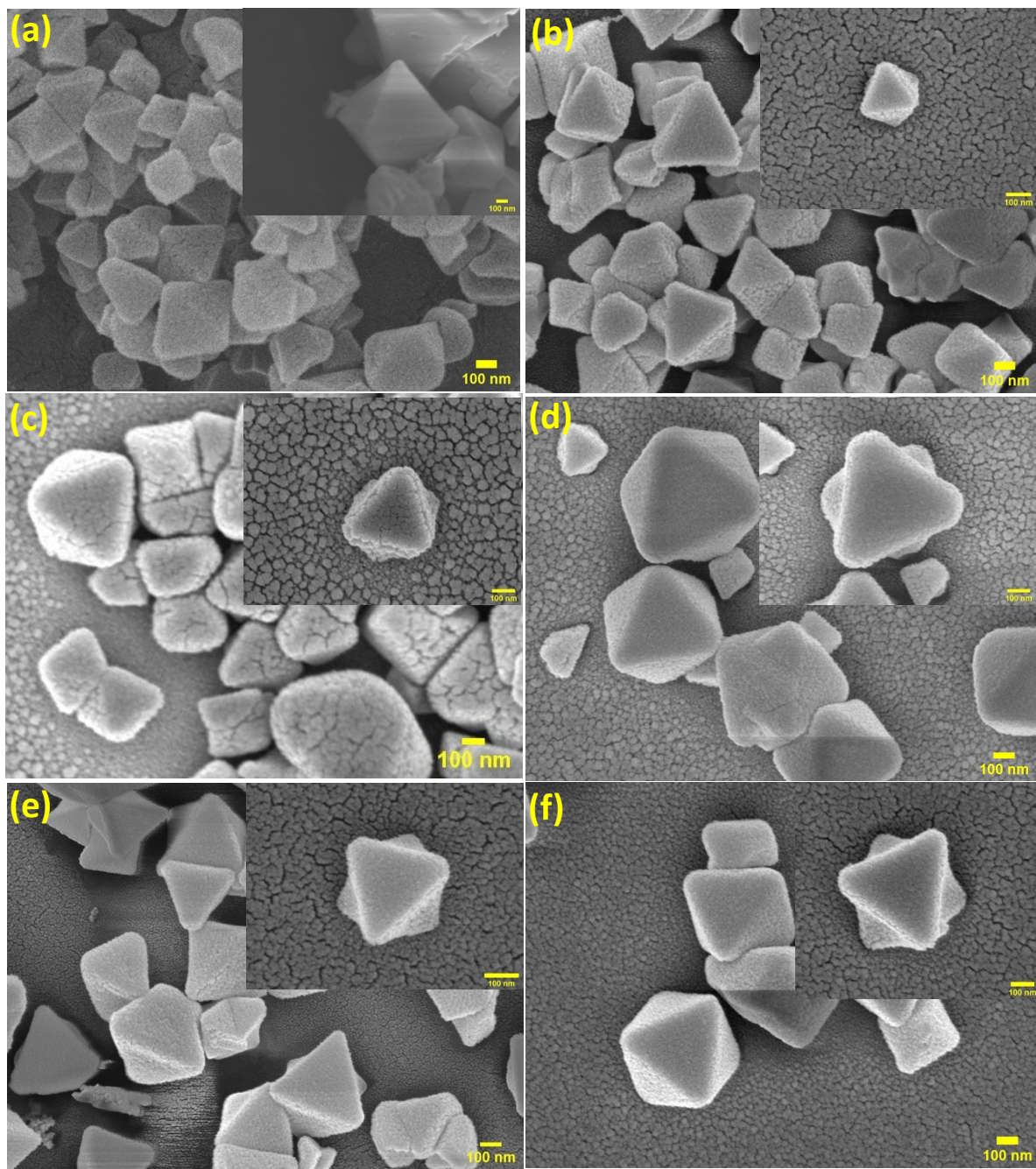
Figure S3. SEM images of (a) MIL-101(Cr), (b) RHA-MIL-101(Cr)-I, (c) RHA-MIL-101(Cr)-II (d) RHA-MIL-101(Cr)-III, (e) RHA-MIL-101(Cr)-IV, and (f) RHA-MIL-101(Cr)-V.
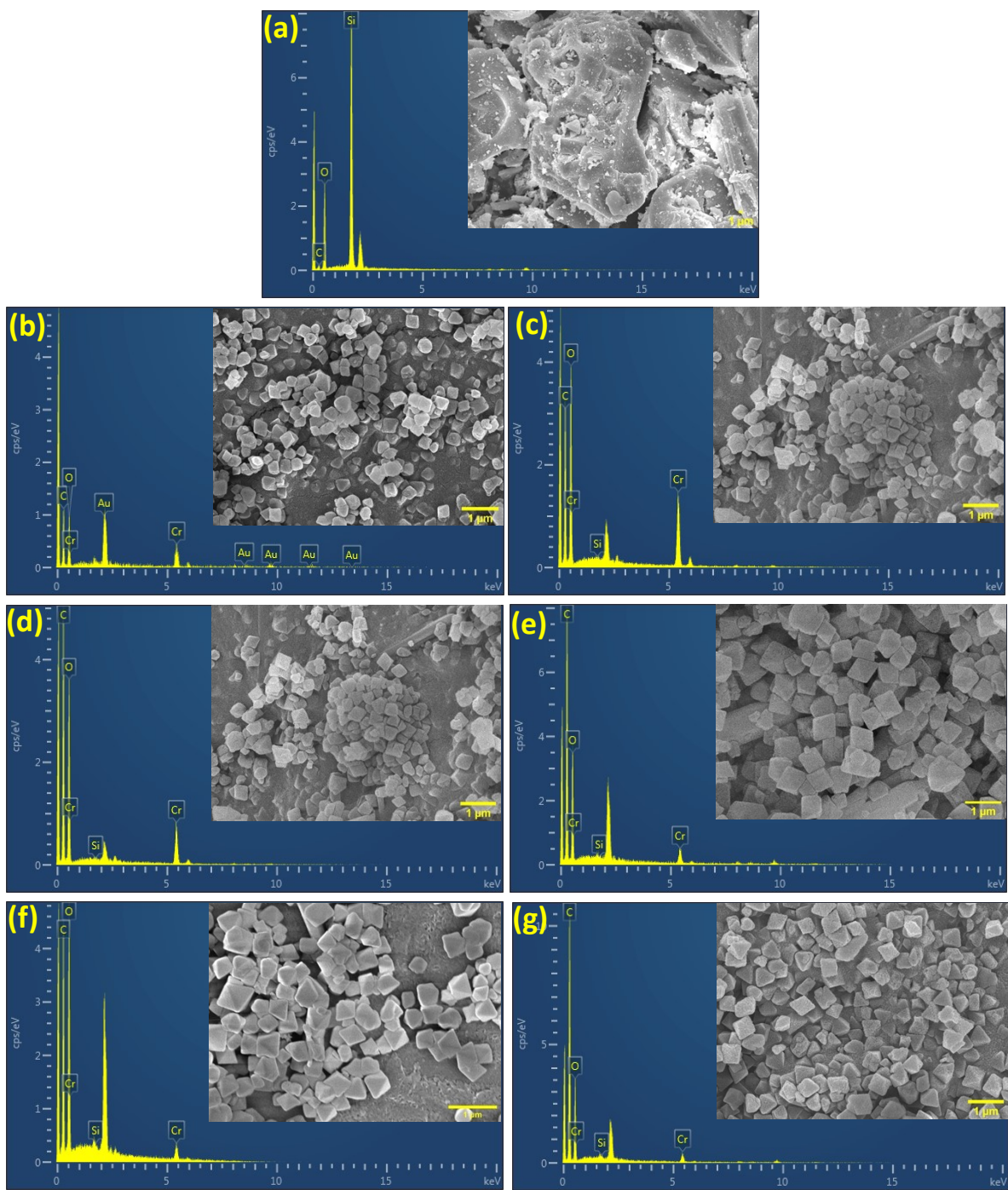
Figure S4. EDS of (a) RHA, (b) MIL-101(Cr), (c) RHA-MIL-101(Cr)-I, (d) RHA-MIL-101(Cr)-II, (e) RHA-MIL-101(Cr)-III, (f) RHA-MIL-101(Cr)-IV, and (g) RHA-MIL-101(Cr)-V.
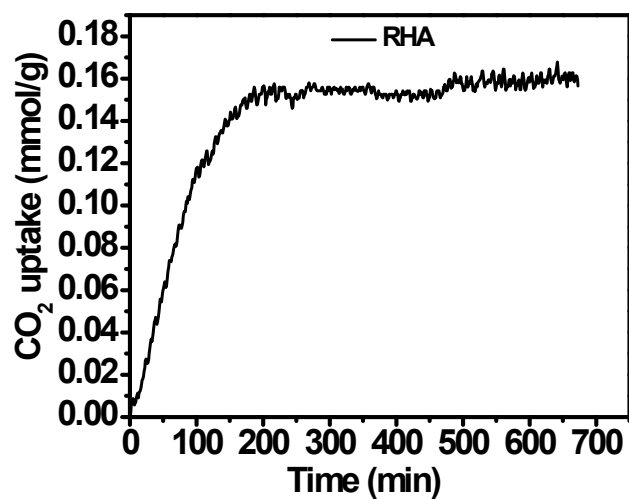
Figure S5. CO_2 adsorption of RHA for 12 h at 30 °C under 400 ppm of CO_2 in He.
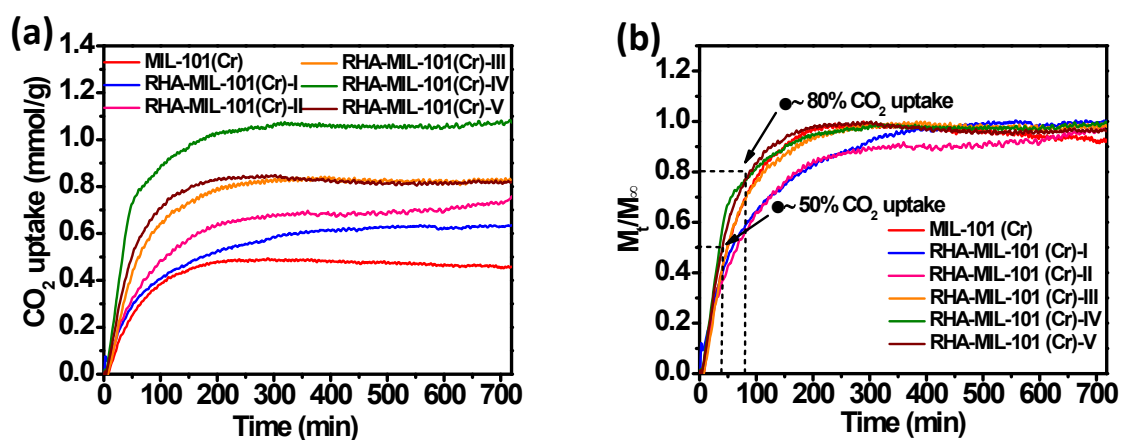
Figure S6. (a) CO_2 uptake profiles and (b) the normalized dynamic CO_2 uptake profiles of MIL-101(Cr) and RHA-MIL-101(Cr) at 30 °C for 12 h under 400 ppm of CO_2 in He.
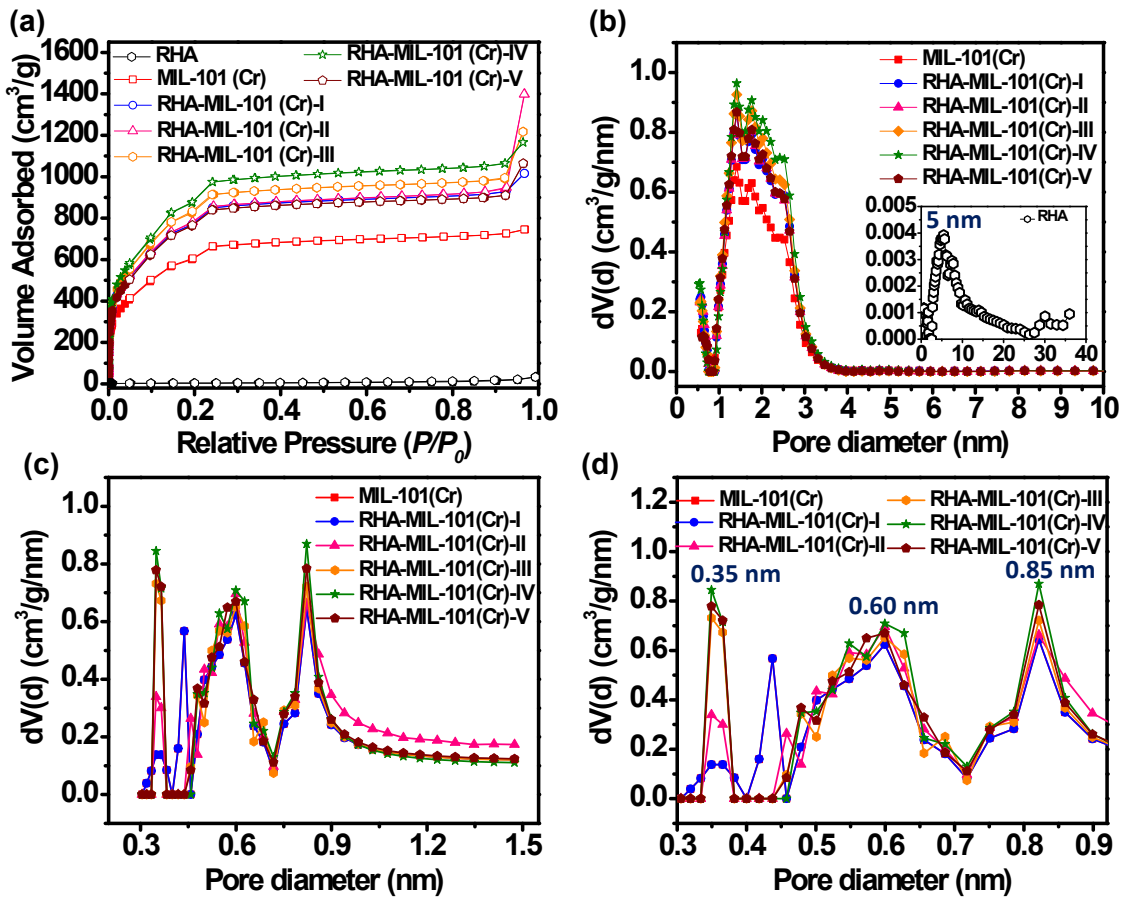
Figure S7. (a) N$_2$ adsorption–desorption isotherms at −196 °C, and (b) pore size distribution of RHA, MIL-101(Cr), and RHA-MIL-101(Cr) obtained from N$_2$ adsorption isotherm. (c,d) micropore size distribution of MIL-101(Cr) and RHA-MIL-101(Cr) obtained from CO$_2$ adsorption isotherm at 0 °C.
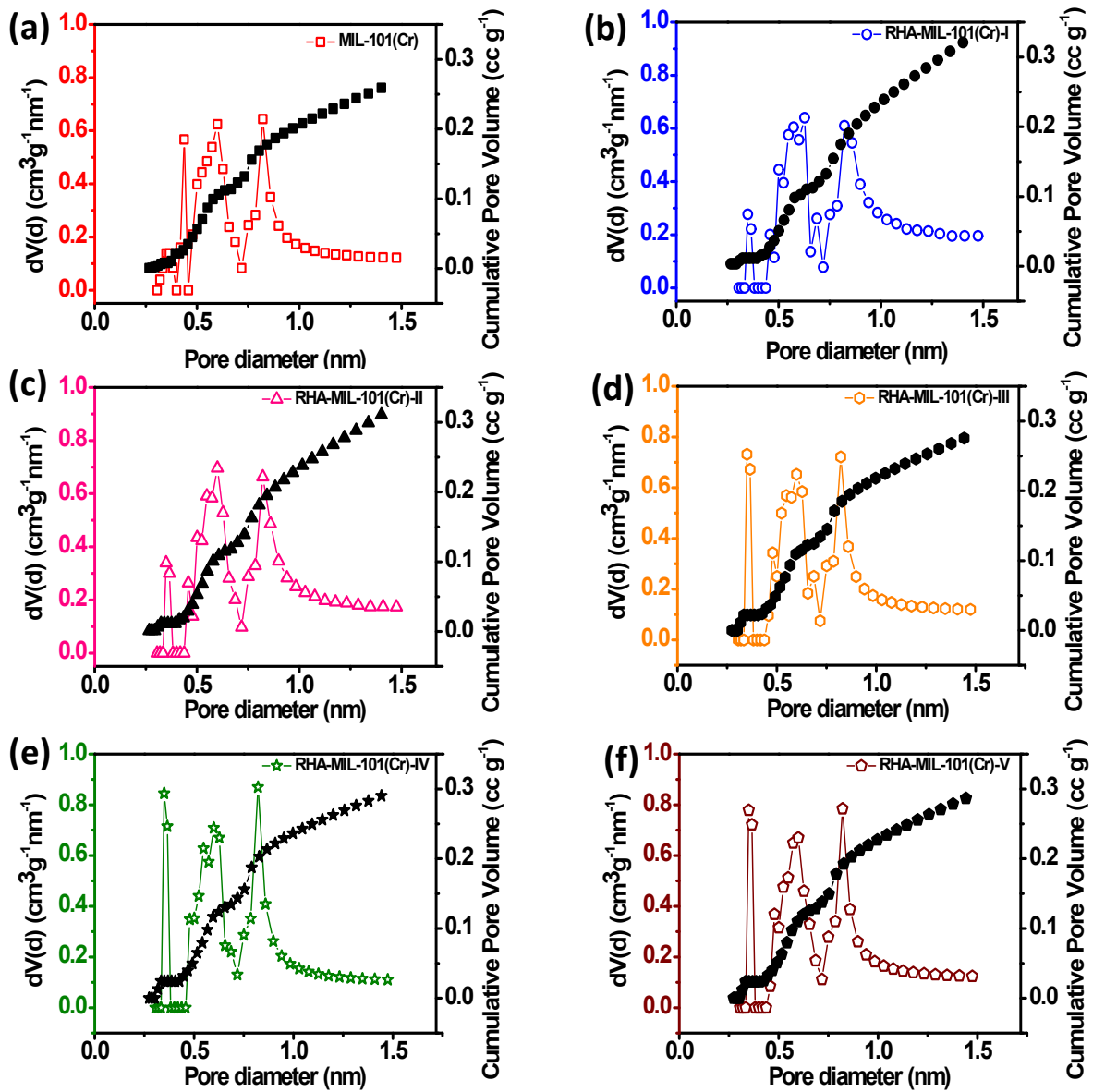
Figure S8. Pore size distribution of (a) MIL-101(Cr), and (b-f) RHA-MIL-101(Cr) calculated from CO_2 adsorption isotherm at 0 ºC.

Materials	S_BET (m²/g)	Pore Volume (cm³/g)		
		V_total	V_micro	V_ultramicro
RHA-MIL-101(Cr)-IV-Powder	3333	1.803	1.362	0.130
RHA-MIL-101(Cr)-IV-Granule	2894	1.666	1.213	0.091
RHA-MIL-101(Cr)-IV-Pellet	2522	1.318	1.018	0.121
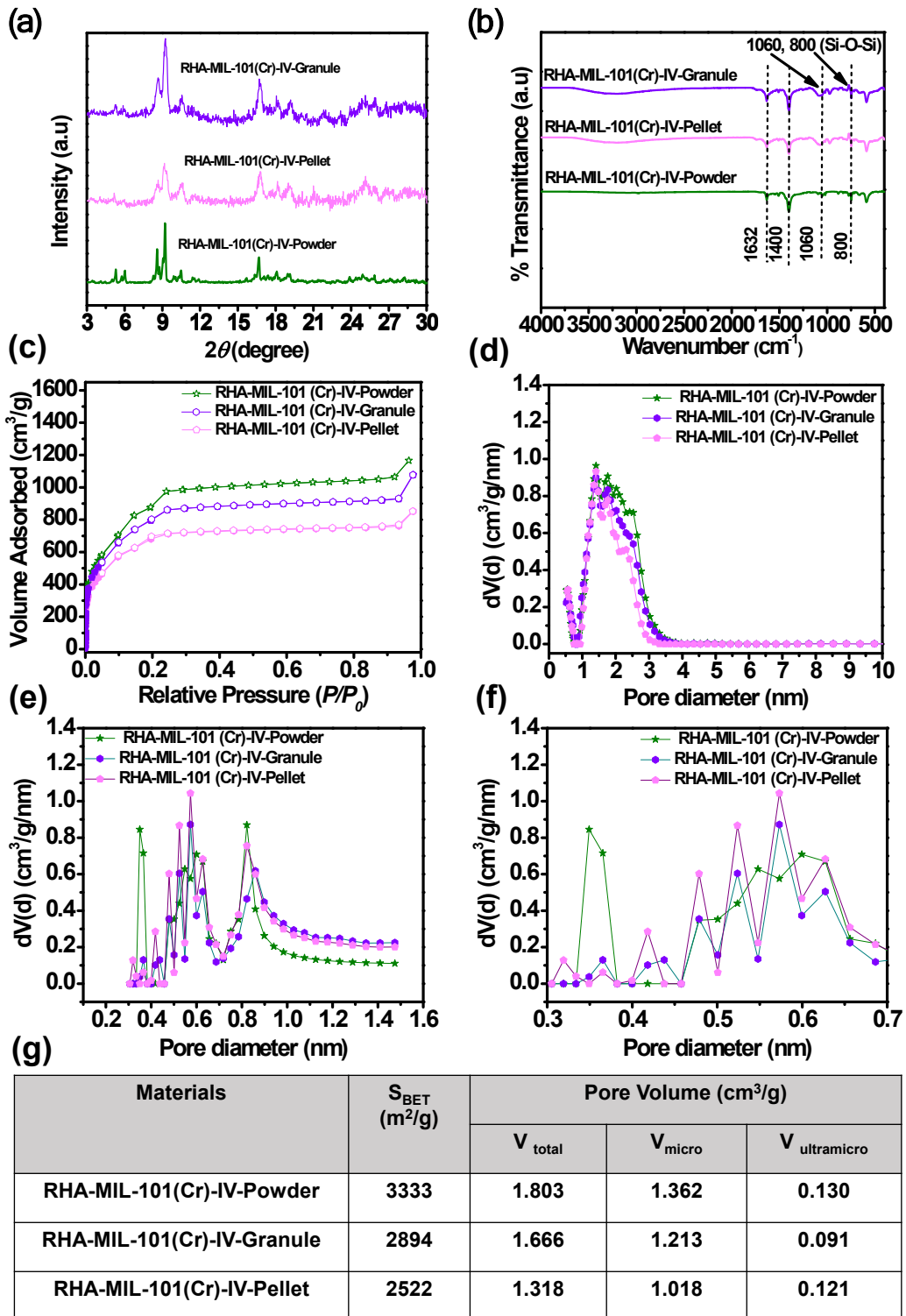
Figure S9. (a) P-XRD pattern, (b) FTIR spectra (c) N_2 adsorption–desorption isotherms at −196 °C, (d) pore size distribution obtained from N_2 adsorption isotherm, and (e,f) micropore size distribution obtained from CO_2 adsorption isotherm at 0 °C, (g) comparative table of textural properties of RHA-MIL-101(Cr)-IV-Powder, RHA-MIL-101(Cr)-IV-Granule, and RHA-MIL-101(Cr)-IV-Pellet.
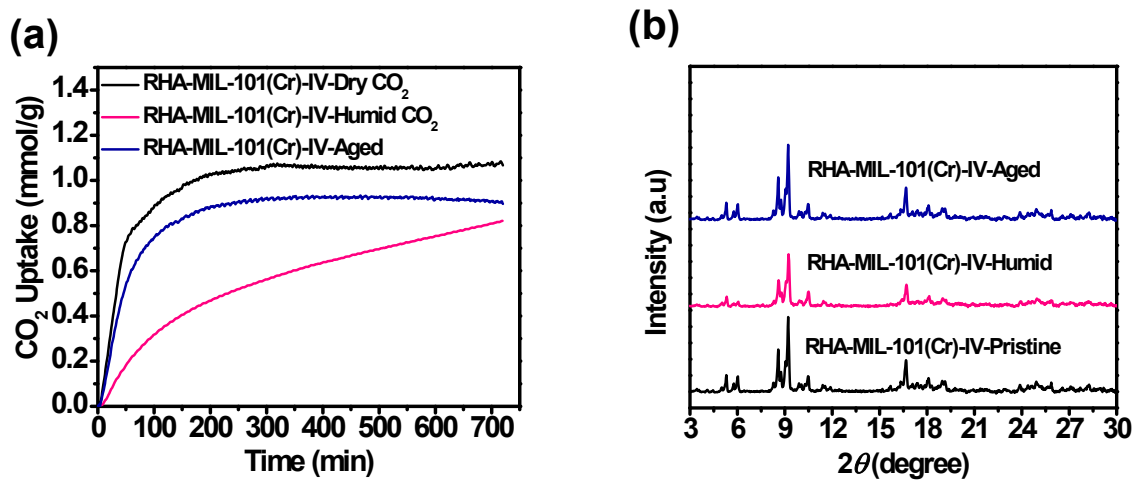
Figure S10. (a) CO_2 uptake under 400 ppm CO_2 at 30°C, and (b) P-XRD patterns of pristine, humid, and aged RHA-MIL-101(Cr)-IV.
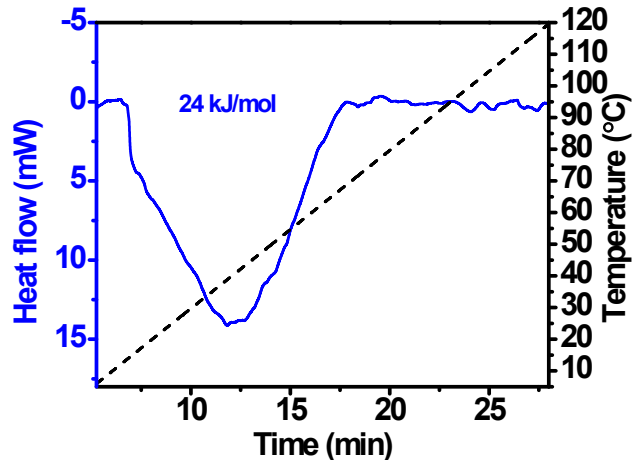
Figure S11. DSC profiles corresponding to desorption of CO_2 from RHA-MIL-101(Cr)-IV.
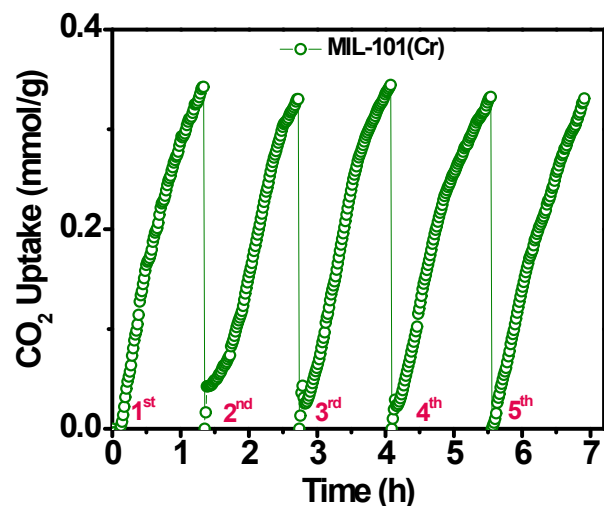
Figure S12. Temperature-swing adsorption (TSA) cycles of MIL-101(Cr) (Adsorption condition: 30 °C for 80 min. Desorption condition: 110 °C for 30 min).

Table S1. Si:Cr ratio obtained from ICP-AES analysis for RHA-MIL-101(Cr).

Element ratio	RHA-MIL-101(Cr)-I	RHA-MIL-101(Cr)-II	RHA-MIL-101(Cr)-III	RHA-MIL-101(Cr)-IV	RHA-MIL-101(Cr)-V
Si:Cr	0.001	0.004	0.008	0.012	0.014

Table S2. Comparative chart of CO_2 adsorption performance of adsorbents under DAC condition.

| Material	Temp. (°C)	CO_2 concentration (ppm)	CO_2 adsorption capacity (mmol/g)	Method	Ref.
Physisorbents					
RHA-MIL-101(Cr)-IV	**30**	**400**	**1.06 (dry) 0.82 (humid)[1]**	TGA	**This work**
SIFSIX-2-Cu-i	25	400	0.07	vol.	[2]
SIFSIX-3-Zn	25	400	0.13	vol.	[2]
SIFSIX-3-Cu	25	400	1.24	vol.	[2]
Mg-MOF-74	25	400	0.08	vol.	[2]
SIFSIX-3-Ni	23	400	0.18	TPD	[3]
HKUST-1	23	400	0.05	TPD	[3]
Mg-MOF-74	23	400	0.14	TPD	[3]
Zeolite-13X	23	400	0.03	TPD	[3]
SIFSIX-3-Cu	23	400	0.32	TPD	[4]
DICRO-3-Ni-i	23	400	0.04	TPD	[4]
SIFSIX-2-Cu-i	23	400	0.04	TPD	[4]
MOOFOUR-1-Ni	23	400	0.06	TPD	[4]
Ni-4-PyC	23	400	0.74	TPD	[4]
DMOF-1	23	400	0.03	TPD	[4]
ZIF-8	23	400	0.05	TPD	[4]
MIL-101	23	400	0.02	TPD	[4]
UiO-66	23	400	0.02	TPD	[4]
NbOFFIVE-1-Ni	25	400	1.30	vol. and TGA	[5]
Zeolite-13X (APG-III)	22	400	0.48-0.51	vol. and GC	[6]
Zeolite NaX	25	395	0.41	vol. and TGA	[7]
Zeolite Li-LSX	25	395	1.34	vol. and TGA	[7]
Zeolite Na-LSX	25	395	0.87	vol. and TGA	[7]
Zeolite Ca-LSX	25	395	0.76	vol. and TGA	[7]
NaY	25	395	0.08	vol. and TGA	[7]
CaY	25	395	0.14	vol. and TGA	[7]
Chemisorbents					
PEI-MIL-101(Cr)	25	400	1.25 (dry) 1.26 (humid)[2]	TGA	[8]
PEI-MIL-101(Cr)	25	400	1.81	vol.	[9]

TEPA-MIL-101(Cr)	25	400	2.14	vol.	9
ED-Mg$_2$(dobpdc)	25	390	2.83	vol.	10
Hydrazine-Mg$_2$(dobdc)	25	400	3.89	TGA	11
ED-Mg-MOF-74	25	400	1.51	TGA	12
mmen-Mg$_2$(dobpdc)	25	390	2.0	vol.	13
TAEA-Cr-MIL-101-SO$_3$H	20	400	1.12	TGA	14

[1]50±3% relative humidity. [2]32% relative humidity (TEPA = tetraethylenepentamine), (PEI = polyethyleneimine), (ED = Ethylenediamine), (TAEA = tris(2-aminoethyl)amine), (mmen = N,N'-dimethylethylenediamine.

vol., volumetric; TGA, thermogravimetric analysis; TPD, temperature programmed desorption

Table S3. Comparative chart of cyclic CO_2 adsorption-desorption stability of various adsorbents for DAC application.

Support	Amine type	Sorbent regeneration condition	Stability performance	Ref.
RHA-MIL-101(Cr)	-	**110 °C for 0.5 h under N$_2$ flow at 20 mL min^{-1}**	**Stable over short multicycle operations (5 cycles)**	**This work**
Silica	PEI	110 °C for 3 h under Ar flow at 100 mL min^{-1}	30.1% capacity loss in 4 cyclic runs	15
Silica	A-PEI	110 °C for 3 h under Ar flow at 100 mL min^{-1}	9.3% capacity loss in 4 cyclic runs	15
Silica	T-PEI	110 °C for 3 h under Ar flow at 100 mL min^{-1}	1.36% capacity loss in 4 cyclic runs	15
Fumed Silica	PEI	85 °C for 3 h under vacuum	3.5% capacity loss in 4 cyclic runs	16
Hierarchical Silica	PEI	110 °C for 6 h under He flow at 100 mL min^{-1}	16% capacity loss in 5 cyclic runs humid condition, whereas no appreciable change in CO_2 adsorption capacity in dry condition	17
SBA-15	PEI	110 °C for 9 h under Ar flow at 100 mL min^{-1}	Stable over short multicycle operations (3 cyclic runs)	18
CA-SiO$_2$	PEI	110 °C for 2 h under He flow	9.6% pseudo-equilibrium capacity and 16% breakthrough capacity loss in 20 cyclic runs	19
Mg$_2$(dobpdc)	en	150 °C for 2 h under simulated air (0.39 mbar CO_2) purge at 60 mL min^{-1}	6% capacity loss in 5 cyclic runs	10
MIL-101-Cr	PEI	110 °C for 3 h under He flow at 90 mL min^{-1}	CO_2 uptake dropped 2.7 % and 1.9% after the first and second cycles, respectively (total 3 cyclic runs)	8
Pore-expanded MCM-41	TRI	100 °C for 3 h by synthetic air at 10 mL min^{-1}	~24% capacity loss in 4 cyclic runs[1]	20

References

(1)   Klinthong, W.; Huang, C. H.; Tan, C. S. Polyallylamine and NaOH as a Novel Binder to Pelletize Amine-Functionalized Mesoporous Silicas for CO_2 Capture. *Microporous Mesoporous Mater.* **2014**, *197*, 278–287.

(2)   Shekhah, O.; Belmabkhout, Y.; Chen, Z.; Guillerm, V.; Cairns, A.; Adil, K.; Eddaoudi, M. Made-to-Order Metal-Organic Frameworks for Trace Carbon Dioxide Removal and Air Capture. *Nat. Commun.* **2014**, *5* (1), 1–7.

(3)   Kumar, A.; Madden, D. G.; Lusi, M.; Chen, K. J.; Daniels, E. A.; Curtin, T.; Perry, J. J.; Zaworotko, M. J. Direct Air Capture of CO_2 by Physisorbent Materials. *Angew. Chem. Int. Ed.* **2015**, *54* (48), 14372–14377.

(4)   Madden, D. G.; Scott, H. S.; Kumar, A.; Chen, K. J.; Sanii, R.; Bajpai, A.; Lusi, M.; Curtin, T.; Perry, J. J.; Zaworotko, M. J. Flue-Gas and Direct-Air Capture of CO_2 by Porous Metal-Organic Materials. *Philos. Trans. R. Soc., A* **2017**, *375*, 20160025

(5)   Bhatt, P. M.; Belmabkhout, Y.; Cadiau, A.; Adil, K.; Shekhah, O.; Shkurenko, A.; Barbour, L. J.; Eddaoudi, M. A Fine-Tuned Fluorinated MOF Addresses the Needs for Trace CO_2 Removal and Air Capture Using Physisorption. *J. Am. Chem. Soc.* **2016**, *138* (29), 9301–9307.

(6)   Wilson, S. M. W.; Tezel, F. H. Direct Dry Air Capture of CO_2 Using VTSA with Faujasite Zeolites. *Ind. Eng. Chem. Res.* **2020**, *59* (18), 8783–8794.

(7)   Stuckert, N. R.; Yang, R. T. CO_2 Capture from the Atmosphere and Simultaneous Concentration Using Zeolites and Amine-Grafted SBA-15. *Environ. Sci. Technol.* **2011**, *45* (23), 10257–10264.

(8)   Darunte, L. A.; Oetomo, A. D.; Walton, K. S.; Sholl, D. S.; Jones, C. W. Direct Air Capture of CO_2 Using Amine Functionalized MIL-101(Cr). *ACS Sustain. Chem. Eng.* **2016**, *4* (10), 5761–5768.

(9)   Rim, G.; Kong, F.; Song, M.; Rosu, C.; Priyadarshini, P.; Lively, R. P.; Jones, C. W. Sub-Ambient Temperature Direct Air Capture of CO_2 Using Amine-Impregnated MIL-

101(Cr) Enables Ambient Temperature CO_2 Recovery. *JACS Au* **2022**, *2* (2), 380–393.

(10)   Lee, W. R.; Hwang, S. Y.; Ryu, D. W.; Lim, K. S.; Han, S. S.; Moon, D.; Choi, J.; Hong, C. S. Diamine-Functionalized Metal-Organic Framework: Exceptionally High CO_2 Capacities from Ambient Air and Flue Gas, Ultrafast CO_2 Uptake Rate, and Adsorption Mechanism. *Energy Environ. Sci.* **2014**, *7* (2), 744–751.

(11)   Liao, P. Q.; Chen, X. W.; Liu, S. Y.; Li, X. Y.; Xu, Y. T.; Tang, M.; Rui, Z.; Ji, H.; Zhang, J. P.; Chen, X. M. Putting an Ultrahigh Concentration of Amine Groups into a Metal-Organic Framework for CO_2 Capture at Low Pressures. *Chem. Sci.* **2016**, *7* (10), 6528–6533.

(12)   Choi, S.; Watanabe, T.; Bae, T. H.; Sholl, D. S.; Jones, C. W. Modification of the Mg/DOBDC MOF with Amines to Enhance CO_2 Adsorption from Ultradilute Gases. *J. Phys. Chem. Lett.* **2012**, *3* (9), 1136–1141.

(13)   McDonald, T. M.; Lee, W. R.; Mason, J. A.; Wiers, B. M.; Hong, C. S.; Long, J. R. Capture of Carbon Dioxide from Air and Flue Gas in the Alkylamine-Appended Metal-Organic Framework Mmen-Mg_2(Dobpdc). *J. Am. Chem. Soc.* **2012**, *134* (16), 7056–7065.

(14)   Li, H.; Wang, K.; Feng, D.; Chen, Y. P.; Verdegaal, W.; Zhou, H. C. Incorporation of Alkylamine into Metal–Organic Frameworks through a Brønsted Acid–Base Reaction for CO_2 Capture. *ChemSusChem* **2016**, *9* (19), 2832–2840.

(15)   Choi, S.; Gray, M. L.; Jones, C. W. Amine-Tethered Solid Adsorbents Coupling High Adsorption Capacity and Regenerability for CO_2 Capture From Ambient Air. *ChemSusChem* **2011**, *4* (5), 628–635.

(16)   Goeppert, A.; Czaun, M.; May, R. B.; Prakash, G. K. S.; Olah, G. A.; Narayanan, S. R. Carbon Dioxide Capture from the Air Using a Polyamine Based Regenerable Solid Adsorbent. *J. Am. Chem. Soc.* **2011**, *133* (50), 20164–20167.

(17)   Kwon, H. T.; Sakwa-Novak, M. A.; Pang, S. H.; Sujan, A. R.; Ping, E. W.; Jones, C. W. Aminopolymer-Impregnated Hierarchical Silica Structures: Unexpected Equivalent CO_2 Uptake under Simulated Air Capture and Flue Gas Capture Conditions. *Chem. Mater.* **2019**, *31* (14), 5229–5237.

(18)   Chaikittisilp, W.; Kim, H. J.; Jones, C. W. Mesoporous Alumina-Supported Amines as

Potential Steam-Stable Adsorbents for Capturing CO_2 from Simulated Flue Gas and Ambient Air. *Energy and Fuels* **2011**, *25* (11), 5528–5537.

(19) Sujan, A. R.; Pang, S. H.; Zhu, G.; Jones, C. W.; Lively, R. P. Direct CO_2 Capture from Air Using Poly(Ethylenimine)-Loaded Polymer/Silica Fiber Sorbents. *ACS Sustain. Chem. Eng.* **2019**, *7* (5), 5264–5273.

(20) Wagner, A.; Steen, B.; Johansson, G.; Zanghellini, E.; Jacobsson, P.; Johansson, P. Carbon Dioxide Capture from Ambient Air Using Amine-Grafted Mesoporous Adsorbents. *Int. J. Spectrosc.* **2013**, *2013*, 1–8.